The Effects of Shear Stress on Angiogenesis in the Skin Microcirculation : In vivo Microscopic Study

皮膚微小血管新生に及ぼすshear stressの効果に関する生体顕微鏡的研究

市岡　滋

The Effects of Shear Stress on Angiogenesis in the Skin Microcirculation : In vivo Microscopic Study

The Effects of Shear Stress on Angiogenesis in the Skin Microcirculation : In vivo Microscopic Study

皮膚微小血管新生に及ぼす shear stress の効果に関する生体顕微鏡的研究

市岡　滋

Contents

Introduction

It is well known that angiogenesis plays the significant role in various fields of medicine. Considerable clinical problems are due to local rarefaction of blood vessels, insufficient neovascularization or both. Impaired placental blood vessel formation results in acute or chronic placental insufficiency, which is an important causative factor for perinatal morbidity and mortality. Necrosis, ulcers, fistulas, and fibroatrophy as the result of decreased vascularization can cause tissue and organ malformation and even the death of the individual. Regular angiogenesis is necessary for uncompromised wound healing and tissue regeneration. Neoplasms growing is governed by angiogenesis of the feeding vessels which often become the targets of nonsurgical therapy of the cancer. Although a variety of the strategies that have been proposed to counteract the deleterious vascularization have been based on the common conviction that acceleration of blood flow improves angiogenesis, the physiological mechanisms responsible for angiogenesis, especially the role of hemodynamic stress generated by blood flow, are not well understood.

The stress-growth principle has been generally accepted in biomechanical and morphological studies. Both soft (Lund and Thomanek, 1978) and hard (Cowin, 1986) tissues accommodate themselves to changes in mechanical stress by remodeling in such a manner as to return the stress to a control point. Blood vessels have also long been known to adapt to the hemodynamic stress induced by blood flow. Since the significant effect of flow-induced stress on vessel growth was initially documented by Thoma (Thoma, 1911), a number of studies have demonstrated that the function and morphology of the vasculature are regulated by hemodynamic stress or wall shear stress. Wall shear stress is a rheological force shearing the luminal surface of the blood vessel when blood flows over the endothelial wall.

By constructing an arterio-venous shunt at the canine carotid artery, Kamiya and

Togawa (Kamiya and Togawa, 1980) first found that sustained increase in the shear stress induced chronic vascular dilatation, so that the stress eventually returned to the control level. Later, Languile and O' Donnel (Langille and O' Donnell, 1986) confirmed that such a shear-induced vascular response was abolished when the endothelium was denuded. These studies have demonstrated that the function and morphology of the large vessels are modified by blood flow or flow-oriented shear stress acting on the vascular wall and that the vascular responses to wall shear stress are endothelium-dependent. They indicated that the adaptive change in vessel diameter against sustained flow load constitute a negative feedback loop regarding the shear stress and constrains the stress constant around its physiological level. More recent in vitro studies using cultured endothelial cells have also revealed that various cell functions, such as proliferative activity during tissue repair and productivity of NO, growth factors and other substances relevant to vascular remodeling are up-regulated by fluid shear stress application, associating concomitant alterations in mRNA expression (Diamond, et al., 1989, Hsieh, et al., 1991, Yang, et al., 1994, Yoshizumi, et al., 1989). In addition, a series of in vitro evidence have established that such shear-induced endothelial cell responses are preceded by internal signal transduction represented by cytoplasmic Ca^{2+} responses (Ando, et al., 1988, Ando, et al., 1991, Ando, et al., 1993).

These in vivo and in vitro findings suggest that angiogenesis in microvessels is most likely affected by wall shear stress. The validity of the assumption that microvessels respond to sustained changes in flow in a manner consistent with maintaining constant shear stress is also verified by the following working hypothesis;

Wall shear stress (τ) is expressed as

$$\tau = 4\mu f / \pi r^3 \qquad (1)$$

where μ, f, r are blood viscosity, blood flow, and vessel radius respectively. Increased blood flow (f) is associated with a proportional increase in wall shear stress (τ) according to the Eq.(1) for Poiseulle flow. When the assumption of the Poiseulle flow

cannot be assumed, particularly in capillaries, stress is established by Stokes formula as follows:

$\tau = (\Delta P/l)(r/2),$ (2)

where $\Delta P/l$ is the gradient of pressure drop. Assuming that the capillary network is a parallel circuit, ΔP is given by

$\Delta P = fR = fR_c/n,$ (3)

where R_c is the resistance of a single capillary, n is the number of capillaries comprising the network, and R is the total resistance of the capillary network ($R = R_c/n$). From Eq. (2) and (3), the formula for τ is written

$\tau = fR_c r/2nl.$ (4)

Eq. (1) and (4) indicate that when flow is increased and if concomitant changes in shear stress induce increase in radius (r), number (n) or length (l) of microvessels, the stress τ is maintained constant. Based on this working hypothesis, it is quite likely that increased shear stress stimulated angiogenesis to form enlarged vascular bed until the shear stress approached the control level, since total vascular volume reflects number (n), length (l), and radius (r) of the vasculature.

In fact, with respect to the skeletal muscle microvasculature, it has been documented that blood flow plays an important physiological role in capillary angiogenesis (Dawson and Hudlicka, 1993, Dawson and Hudlicka, 1989, Hudlicka, et al., 1992), because sustained increase in peripheral blood flow in muscles caused by repeated electrical nerve stimulation or by chronic prazosin administration stimulated capillary angiogenesis and increased capillary density, while reduced peripheral blood flow caused the size and number of arteriole to decrease (Wang and Prewitt, 1991). However, direct experimental evidence, manifesting the role of wall shear stress in microvascular angiogenesis, has not been presented probably because of inherent technical problems associated with chronic in vivo studies.

Purpose

In this study, we have attempted 1) to visualize by quantitative data, how effectively the increased peripheral blood flow by chronic administration of α-1 blocker, prazosin, enhances the microvascular angiogenesis during tissue repair in the rabbit ear chamber which provides an excellent means of observing and quantifying wound-healing angiogenesis, and 2) to elucidate whether the adaptive responses of microvasculature to increased wall shear stress is involved as the key mechanism of the observed phenomenon or not. These aims were achieved by repeating non invasive microscopic observation and video recording of the microcirculation in the regenerated tissue in the chamber and by assessing changes in the shear stress level with time at venules from recorded images. The recording was carried out in conscious animals, starting approximately one week after the chamber implantation and was continued bi-daily until the repairing process was completed within 3 to 4 weeks.

Materials and methods

Animals and anesthesia

Male Japanese White rabbits weighing 3.2-3.5 kg were used. The ear chamber was installed under the anesthesia of 40 mg/kg ketamine by intramuscular injection combined with local anesthesia induced by 8% lidocaine spray. All observations of the microcirculation in the ear chamber were carried out under unanesthetized animal placing in a restraining holder. The rabbits were housed one per cage, kept under a constant environmental temperature of 25℃ and fed a commercial rabbit chow.

Implantation of the rabbit ear chamber

The chamber, made of transparent acryl-resin, is composed of a disk with a central round table and three marginal pillars, a cover plate and a holder ring, as usually used for vital microscopic observation of the microcirculation (Asano, et al., 1963). On the cover plate, a grid is printed to divide the central part into 10x10 sections (500 μm in each side length) for accurate allocation of the microvasculature in the observation window (6 mm in diameter) (Fig. 1). The ear was shaved, treated with a depilatory cream and sterilized with povidone-iodine. Four holes were punched through the cartilage and skin of the distal portion of the ear with a specially designed puncher. The size and position of the holes were adjusted to match those of the round table and pillars of the disk (Fig. 2A). Care was taken to avoid large blood vessels. The epidermis on both sides of the ear around the central hole was carefully retracted so as to leave the subcutaneous blood vessels intact (Fig. 2B). Three peripheral pillars of the disk were inserted through the outer small holes of the ear to position the chamber and the central round table plugged the large puncture in the center. A cover plate was fixed on the pillars by the holder ring (Fig. 2C). The disk was designed to leave a 50-μm-thick and 6-mm-diameter gap between the central round table and the cover plate. This space formed a cavity into which newly sprouting microvessels could grow from the vessels of the subdermis and the cavity was filled with saline (Fig. 3). An antibiotic, gentamicin suspension (2 mg) was

injected intramuscular after the procedure.

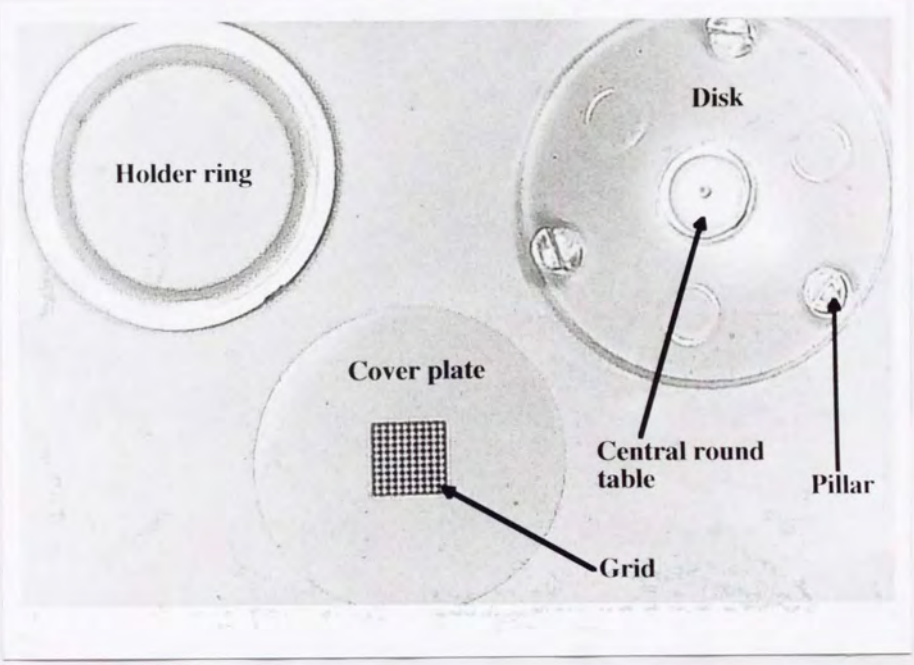

Fig. 1: Complete rabbit ear chamber set . The chamber is composed of a disk with a central round table and three peripheral pillars, a cover plate, and a holder ring. A 10 x 10 grid (grid constant 500 μm) is printed on the cover plate.

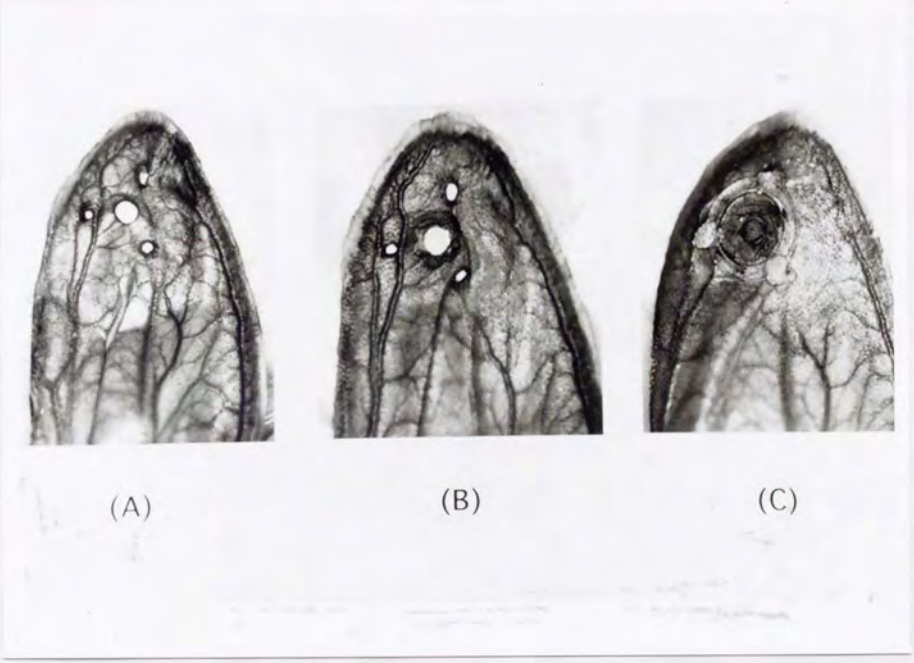

Fig. 2: Surgical procedure for implantation of the rabbit ear chamber. (A) Three outer holes and a central puncture in the distal portion of the ear. (B) The epidermis on both aspects of the ear around the puncture is carefully retracted. (C)The ear chamber installed.

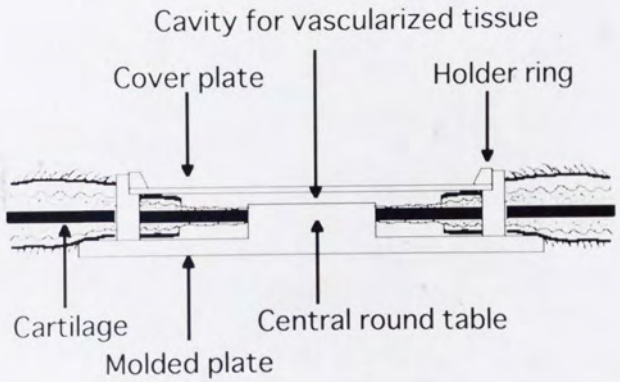

Fig. 3: Schematic representation of rabbit ear chamber. The central dead space is sandwiched between the molded plate and cover glass to form the cavity (50 μm x 6 mm). The growing granulation tissue sprouts into the space.

Administration of prazosin

The α-1 blocker prazosin hydrochloride (Pfizer) was used as a vasodilator, accordingly to previous reports (Dawson and Hudlicka, 1989, Price and Skalak, 1996). A saturated solution of prazosin hydrochloride in distilled water at room temperature (approximately 100 mg/l) was prepared. The solution was diluted to 50 mg/l with water. Rabbits (n = 6) received solution of prazosin (50 mg/l in water), to drink ad libitum from 0 to 23 postoperative day (POD). Rabbits drank about 200 ml of the solution. The control group (n = 8) was supplied with distilled water for the same period. The consumption of fluid was similar in the two groups. Plasma concentration of the drug was measured by a fluorescence spectrography (F-3010 Hitachi, Japan) from blood samples in rabbits on 23 POD.

In vivo microscopic observation and video recordings

The ear chamber was examined every day from 4 to 8 POD to find the first appearance of the new vessels. Then the chamber was inspected every second day from 9 to 23 POD in a stereo microscope (SZH 10, Olympus, Japan) coupled with a CCD (charged coupled device) color video camera (DXC-107 A, Sony, Japan) (Fig. 4). To achieve sufficient transillumination of the tissue in the ear chamber, a 150W halogen projection lamp (Nikon) was used as a light source which allowed the imaging at a shutter speed of 1/10,000 second on a video recorder (SLV-RS1, Sony, Japan). Such high shutter speed was needed to measure red blood cell velocity by using the dual-window method described later, because this method required good contrast between the moving red blood cells and the surrounding plasma. The images of an entire observation window were recorded at low magnification followed by separate recording of the images for every square in the grid together with time and frame counts (VTG-33, FOR. A, Japan) for the later analysis at high magnification. The final magnification on the video monitor was x 550.

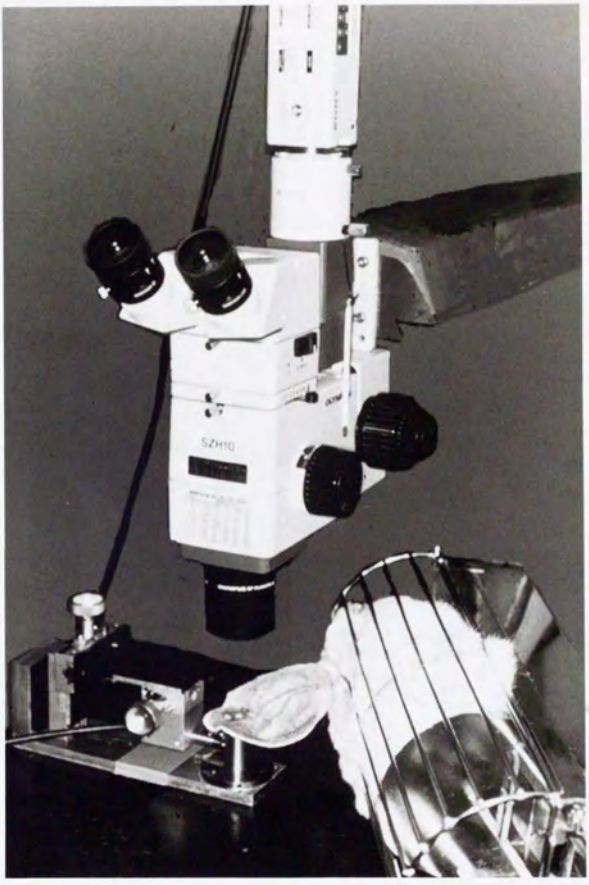

Fig. 4: Observations of the ear chamber were made without anesthesia by placing the rabbit in the restraining holder. The ear chamber is maintained in position by screw clamp under a stereo microscope fitted with CCD color video camera.

Evaluation of vascular ingrowth area

A computerized image analysis system software (Image 1.44 NIH) and a personal computer (Macintosh Quadra 840 AV, Apple, USA) were employed for quantifying the recorded images. The recorded video images of the entire window were displayed on the monitor by graphic software (Adobe Photoshop Ver.2.5) as a digitized gray-scale image (8 bits/pixel). Vascular ingrowth was seen in the form of well-defined vascular sprouts forming a "vascular front" (Fig. 5). The advancing edge of the "vascular front" was traced and the peripheral area occupied by vascularized tissue was painted with a paint function by referring to the video images. The painted image was converted to the binary image by using thresholding function of the image analysis software. Thresholding of a gray-scale image produced a two-color (black and white) image in which all pixels having a gray level less than or equal to the threshold value are set to black and all pixels having a gray level greater than the threshold are set to white. In the final binary image, vascularized tissue exhibited white and non-vascularized area revealed black. The gray level intensity (I) of white (vessels) was 255 and the I of black (background) was 0.

The relative area of the window covered by vascularized granulation tissue (CA) was calculated from the mean gray level intensity (GL) of the image by

$$CA = (GL/255) \times 100 \qquad (5)$$

The results were expressed as percentages of the wound chamber filled with repairing tissue. The vascular ingrowth rate (mm^2 / day) was also calculated from the slope of the relative area curves.

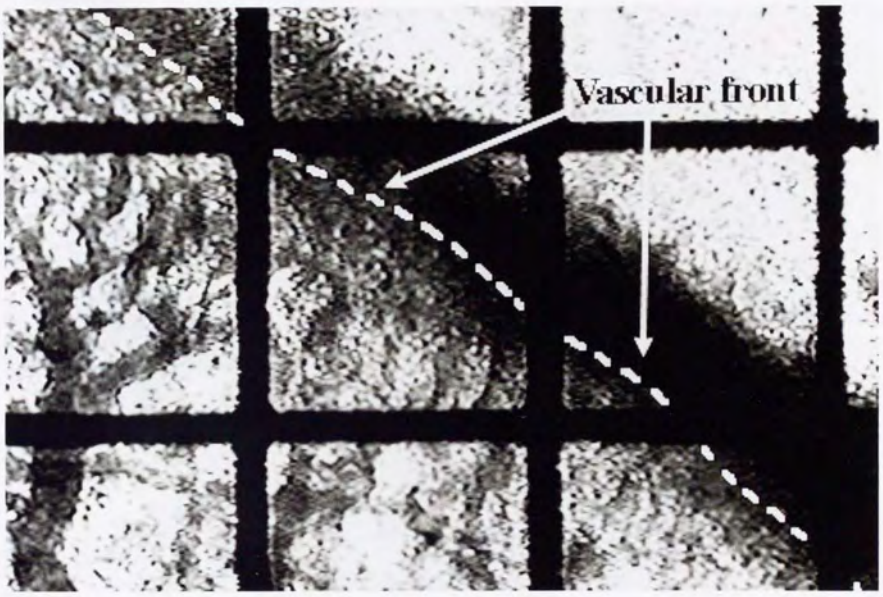

Fig. 5: A dotted line marks the "vascular front" i.e. a boundary between the vascularized granulation tissue and the dead space.

Morphometric estimation of the vasculature

The image of the microcirculation in each section in the grid was digitized and stored in the computer as a 32-bit/pixel RGB color image file (Fig. 6 A). In order to demarcate blood vessels from background tissue, the vascular regions in each image were accurately traced by means of white paint function (Fig. 6 B). As some small capillaries were difficult to be identified in the freeze-captured image, we also used the replay of the original moving image to confirm the capillary channel from the movement of red blood cells in capillaries. The original image was subtracted from the traced image (Fig. 6 C). The binary threshold level was determined with thresholding function of the software so that, in a final binary image all the vessels were collared to white (I: 255) on a black background (I: 0) (Fig. 6 D).

The laborious procedure of tracing the vascular regions was essential to obtain idealized binary images from which fractional areas covered by blood vessels were quantitatively evaluated. Precise binary images required good contrast between blood vessels and background tissue.

From the binary images thus obtained for all sections, we calculated the following parameters : 1) The number of sections occupied by vascularized tissue (N). 2) The mean gray level intensity of each section (MG_i) reflecting the relative area occupied by blood vessels in the section. 3) the mean vascular density (MD) as the fractional area of the image covered by white blood vessels per mm^2 in the covered area.

$$MD = \sum_{i=1}^{N} (MG_i) / N / 255 \qquad (6)$$

4) The relative area of the total vascular bed (RA) denoting the fraction of the area covered by blood vessels in the chamber was estimated by; $RA = CA \times MD$. (7)

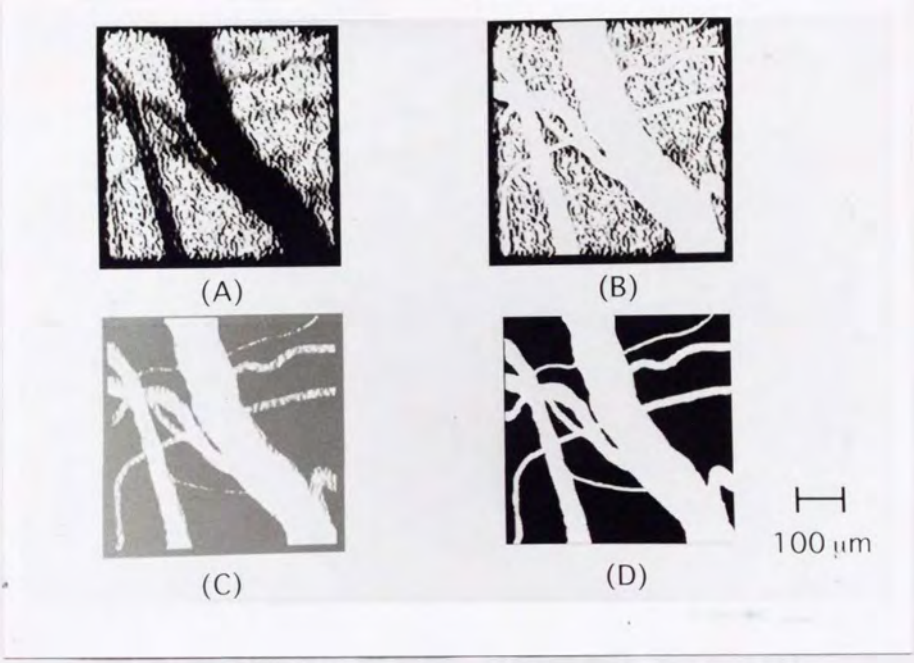

Fig. 6: Processing steps for a microvascular digital image. (A) Original image. (B) Traced image where the vascular regions were painted white. (C) Subtracted image. (D) Resulting binary image that had white vessels on a black background.

In vivo assessment of wall shear stress in venules

For quantification of wall shear stress in microvessels, the velocity of red blood cells and diameter of individual venules were measured on 9, 13 and 21 POD. The venules which had diameter of 20-40 μm were chosen for the analysis.

The velocity of red blood cells through individual vessels was determined by dual-window method (Intaglietta, et al., 1975) using a photometric image processing and measuring system (C5003 Hamamatsu Photonics, Japan). In this method the time delay between the video signals which originate from two windows positioned along the image of a microvessel was measured by an off-line cross-correlation technique (Fig. 7). Video signals were sampled every 500 msec for 30 sec at the windows overlaying a sampled venule. The photometric windows were generated directly within the composite video signals, and were positioned by means of manual analog controls. The upper limit of the red cell velocity measurement in this method was limited by the framing rate of the video system to a maximum velocity of about 2 mm/s (Johnson, 1986). The venules of which velocity exceeded this upper limit were actually very seldom. Venular diameters were measured on video pictures with the calibrated ruler function of image-analyzing software.

Using the value of velocity (v) and the radius (r) of each venule, shear stress (τ) was given by assuming Poisuelle's flow as

$$\tau = 4\mu v / r \qquad (8)$$

Blood viscosity (μ) was assumed constant during the experiment as $\mu = 3 \times 10^{-2}$ dyne $\cdot$ s / cm^2 from the reported data (Baba, et al., 1995). The average of all the calculated shear stress in sampled venules was taken as the representative value at each measuring day. The number of venules per animal adopted for the measurement was 10.7 $\pm$ 0.67, 16.0 $\pm$ 0.58 and 21.3 $\pm$ 0.88 (mean $\pm$ SEM) on 9, 13 and 21 POD, respectively.

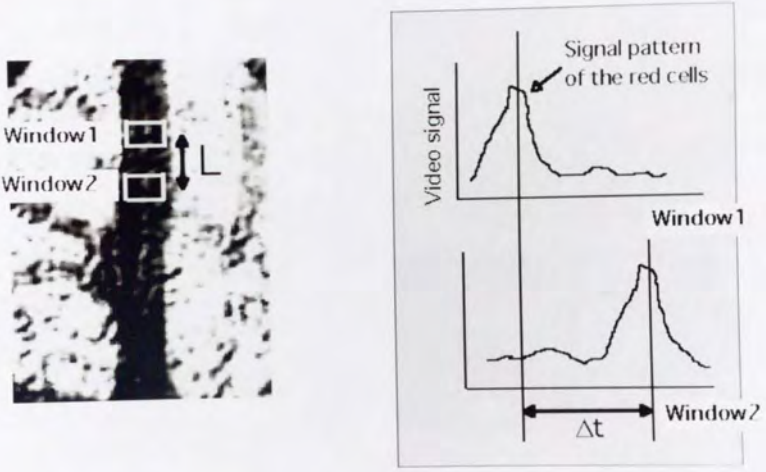

Fig. 7: The principle of the dual-window method. A characteristic signal pattern is generated by the train of red cells as they pass under the upstream window (window 1) and this pattern is very closely reproduced at the nearby downstream site (window 2) . The time delay (Δt) can be determined by comparing the two patterns using a correlation technique. Red cell velocity (v) is given as $v = L/\Delta t$ where L is the distance between the two windows.

The pharmacological effect of prazosin on the endothelial cell proliferation

To investigate a direct pharmacological effect of the drug on endothelial cell proliferation, the growth curve of endothelial cells in the culture medium was examined under 2 different concentrations of prazosin (15 ng /ml and 150 ng / ml). HUVECs were isolated from collagenase treated human umbilical veins. Cells were cultured in medium 199 with 15 % fetal bovine serum, 100 μg / ml endothelial growth supplement, 50 μg / ml heparin, 2 mM glutamine, and an antibiotic cocktail of 100 U / ml penicillin and 100 μg / ml streptomycin. Endothelial cells were seeded at 1 x 10^4 cells / cm^2 in a 24-well dish (2.0 cm^2/well) and incubated in control and prazosin-added medium. The selected concentration of prazosin was assessed based on the data of plasma concentration of the drug measured by a fluorescence spectrography from blood samples in rabbits during the daily oral administration. One, 3, 5 and 7 days after seeding, the number of cells was counted using a Coulter counter (Model ZM, Coulter electronics, UK) and expressed as cell density (cells / well).

Acute effect of prazosin

The acute vasodilating effect of prazosin was confirmed in the ear chamber at 27 POD in untreated rabbits under intraperitoneal Urethane anesthesia (1 g/kg). After cannulating the external jugular vein for infusion and the femoral artery for arterial pressure and heart rate monitoring, a prazosin solution was slowly infused for 60 min. The infusion rate was selected to attain the dose of about 5.0 μg/kg, to match the plasma concentration of the drug during oral administration.

Statistical analysis

To compare the mean values of the two groups at each observation day, statistical significance of the differences was tested by Student's unpaired t test. A difference at the

5% level was considered significant and indicated with an asterisk. The values are given as means ± SEM.

Results

Plasma concentration of prazosin

The mean plasma concentration of prazosin after oral administration for 23 days was 70.17 ± 20.0 ng/ml in prazosin-treated rabbits.

The relative covered area (CA)

After the operation, the chamber was filled with cellular debris consisting of floating cells and fluid resulting from the surgical procedure. Sprouting vessels always originated from preexisting vessels immediately adjacent to the debris. The new vessels first appeared at the periphery of the chambers significantly earlier in the prazosin-treated animals than control. Vessel growth progressed from the periphery concentrically toward the center until the chamber was filled. The first appearance of the vessels in the chamber was 6.5 ± 0.61 POD in prazosin-treated group and 8.6 ± 0.51 POD in control group ($P < 0.05$). The area covered with vascularized tissue increased with time in a sigmoidal way and all chambers in both groups were entirely covered by 21 POD. It took an average of 21.3 ± 0.59 days for the chamber of the control animals to be completely covered with vascularized tissue versus 17.3 ± 0.33 days for the treated animal. The difference was highly significant ($P< 0.001$). CA values in the prazosin-treated group were significantly higher than those in the untreated group throughout the period from 7 to 19 POD (Fig. 8) (Fig. 9). The ingrowth rate of the vascularized tissue in the chamber was significantly greater in treated group than the control group during 7 to 11 POD (Fig. 10).

The mean vascular density (MD)

MD values in the prazosin treated group showed significantly higher levels than those of the control group during the periods from the 11 to 23 POD except 17 POD (Fig. 11).

The relative area of the total vascular bed (RA)

Fig. 12 shows the calculated results of RA from CA and MD data by Eq. (7). RA gradually increased with time as CA did. RA values in the prazosin-treated group were all significantly greater than those in the control group throughout the entire period of observation. The final RA value in the treated group was approximately 21% larger than that in the control group. As is seen in Fig. 13, the general appearance of the microvasculature at the final stage revealed that the chamber in the treated group was more densely vascularized by vessels with larger diameter than that in the control group.

Wall shear stress in venules

As shown in Fig. 14, venular diameters showed no significant difference between two group because the vessels in a limited range of diameter (20-40 μm) were selected for red cell velocity measurement. Initial blood velocity on 9 POD in prazosin-treated and control chambers was 0.30 ± 0.060 mm/s and 0.21 ± 0.022 mm/s respectively (NS; P=0.217) (Fig. 15). The wall shear stress calculated by Eq.(8) exhibited significantly elevated value in the treated group (2.48 ± 0.27 dyne/cm^2) than in the control (1.55 ± 0.26 dyne/cm^2) ($p<0.05$). The flow velocity in the treated group was reduced from 9 to 13 POD while the velocity in the control group did not differ significantly among the three measuring day (Fig. 16). A similar tendency was revealed in wall shear stress values, although the difference between the prazosin treated and control group was not significant in 13 and 21 POD data.

The growth curve of HUVECs in the medium of different prazosin concentration

Fig. 17 shows the growth curves of HUVECs obtained in the three culture medium containing prazosin in the concentration of 0, 15 and 150 ng / ml. The curves revealed no significant difference at any days. The direct effect of prazosin on HUVEC proliferation was not positive.

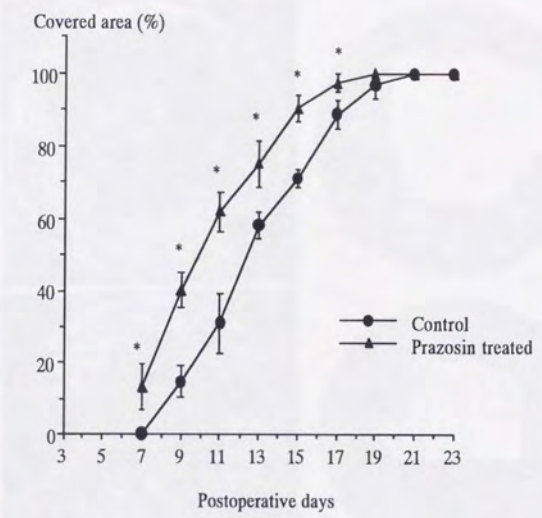

Fig. 8: Relative area of the chamber covered with vascularized tissue (CA) expressed as percentages in the control (n = 8) and the prazosin treated group (n = 6). * Significantly different at $p < 0.05$.

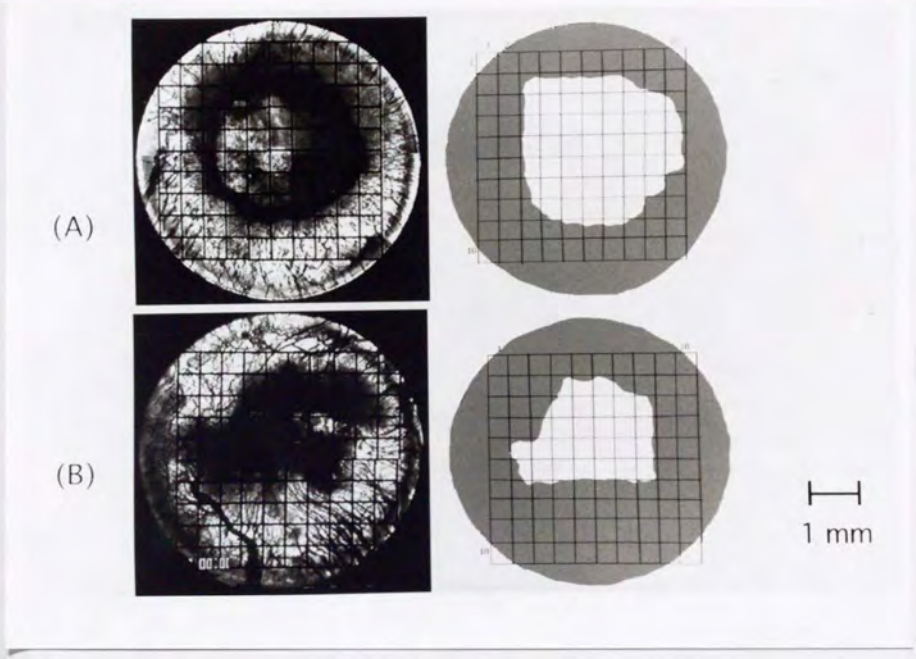

Fig. 9: Microscopic appearance of the chambers on postoperative day 13 . (A) Representative control and (B) prazosin-treated animal. The advancing edge of "vascular front" is traced and the peripheral area has been painted. Note that the microvasculature in the treated animal proceeded more rapidly and densely.

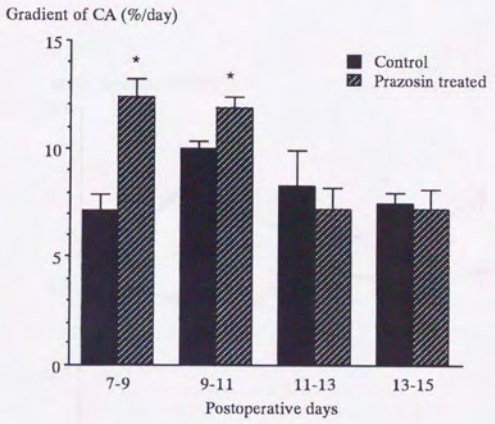

Fig. 10: Ingrowth rate of the vascularized tissue in the chamber calculated from the gradient of CA curves. * Significantly different at $p < 0.05$.

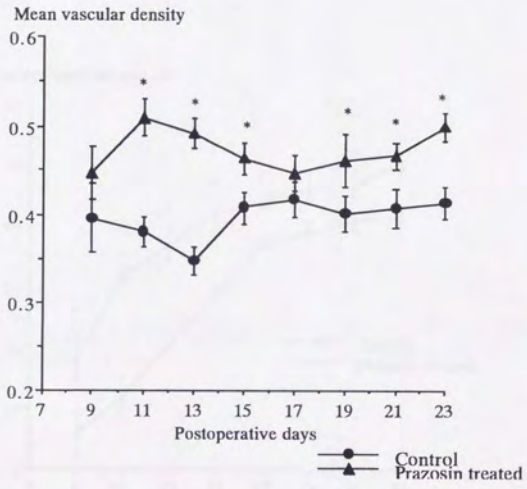

Fig. 11: Mean vascular density (MD); the fractional area covered by blood vessels per mm^2 in control and prazosin-treated animals. *Significantly different at $p<0.05$.

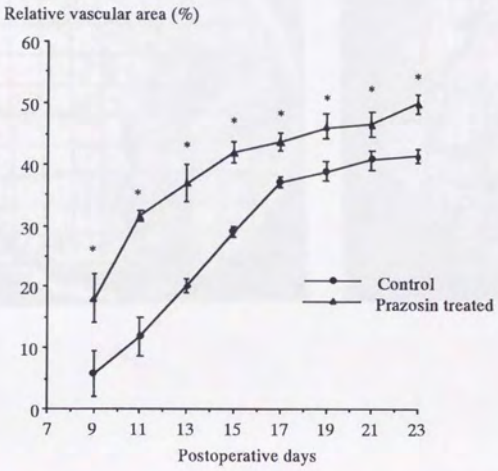

Fig. 12: Relative vascular area (RA); the fraction of the area covered by vessels in the chamber. *Significantly different at $p < 0.05$.

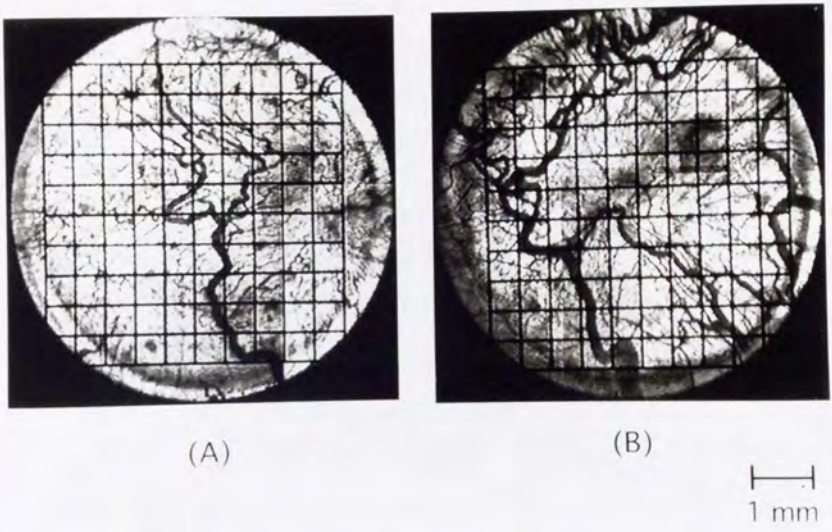

Fig. 13: General appearance of the microvasculature in the chamber. (A) The gross view of the chamber at low magnification in the representative control and (B)treated animals on 19 POD. Note that the microvascular structure was composed of a dense vascular network in the treated chamber.

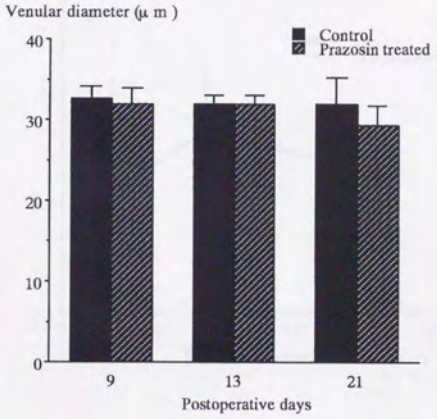

Fig. 14: Diameter of venules sampled for measurement of red blood cell velocity.

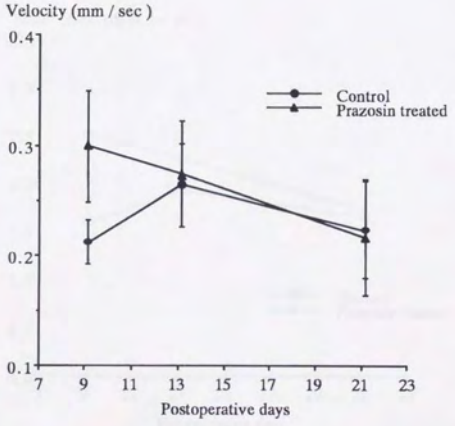

Fig. 15: Velocity of red blood cell in venules (diameter in 20 - 40 μm).

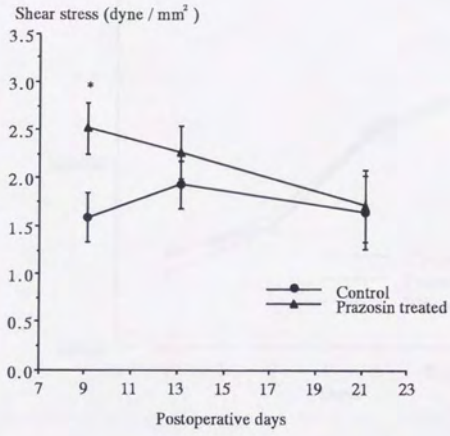

Fig. 16: Changes in wall shear stress in venules on day 9, 13 and 21 in the control (n = 4) and the prazosin treated group (n=4). *Significantly different at $p<0.05$.

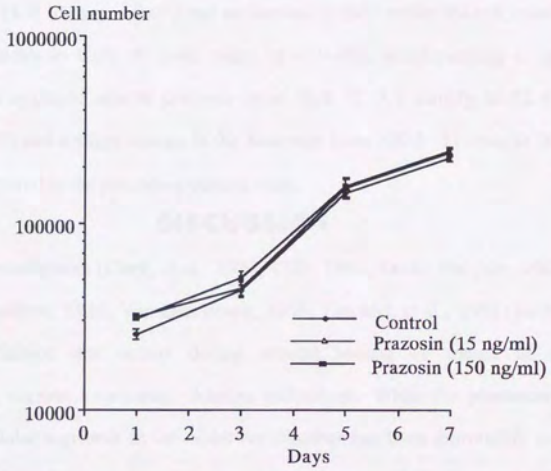

Fig. 17: Growth curves for HUVECs cultured in a 24-well dish. Cell counts have been plotted versus the number of days with or without prazosin. No significant difference was observed. n= 3 for each dot.

Acute effect of prazosin

The microscopic video image analyses following intravenous infusion of prazosin (50 μg/kg) revealed a moderate enlargement of the venule diameter from 40.7 $\pm$ 10.2 μm to 53.4 $\pm$ 14.8 μm ($p < 0.05$) and an increase in the venular red cell velocity from 0.19 $\pm$ 0.01 mm/s to 0.26 $\pm$ 0.02 mm/s ($p < 0.05$), accompanying a significant reduction in the systemic arterial pressure from 76.8 $\pm$ 3.6 mmHg to 52.4 $\pm$ 1.0 mmHg ($p < 0.05$) and a slight change in the heart rate from 329 $\pm$ 11 /min to 307 $\pm$ 8 /min (NS), compared to the preceding control state.

DISCUSSION

Several investigators (Clark, et al., 1931, Cliff, 1965, Dudar and Jain, 1983, Ebert, et al., 1939, Sandison, 1928, Van Den Brenk, 1956, Zawicki, et al., 1981) have studied the neovascularization that occurs during wound healing by means of intravital microscope and various transparent chamber techniques. While the phenomenological processes of cellular ingrowth in the rabbit ear chamber has been thoroughly evaluated, the physiological mechanisms regulating angiogenesis, especially the potential role of hemodynamic stress as a determinant of vascular structure, have not sufficiently studied in vivo. The results of this study showed that angiogenesis during wound healing in the rabbit ear chamber is positively influenced by administrating the α1-adrenergic blocker prazosin to modify microvascular hemodynamics.

The treatment protocol used for prazosin administration in previous studies (Dawson and Hudlicka, 1989, Price and Skalak, 1996, Ziada, et al., 1989) was chosen. Although it is generally recognized that the events in the microcirculation provoked by the vasodilator prazosin are due to changes in hemodynamic stress resulting from increased blood flow (Hudlicka, et al., 1992), several mechanisms other than the hemodynamic change that we suspect are possible. Price and Skalak (Price and Skalak, 1996) assessed

biochemical effects of prazosin treatment, including changes in tissue oxygenation, potential effect on angiotensin II levels, and the direct effect on smooth muscle growth. They carefully excluded these potential effects from factors facilitating microvascular formation, referring to the related literature in detail. On the other hand, it has been reported that vasodilators significantly increased red blood cell velocity (Tillmans, et al., 1977), dilated terminal arterioles (Tillmans, et al., 1984), and slightly increased pressure in the venule (Tillmans, et al., 1981). It was also observed in this study that administration of prazosin increased the peripheral blood flow in the microcirculation during wound healing. Furthermore, we investigated the direct chemical effect of prazosin on endothelial cell proliferation to eliminate the possibility that the drug directly promoted vascular growth. The results in Fig. 17 clearly denied the possibility that prazosin itself is a stimulant of proliferative activity of the endothelial cells. This finding is consistent with the results in conventional studies concerning relevant effects of most vasodilators. Hence, the observed phenomena in this study induced by the prazosin treatment can be regarded as the consequence of its vasodilating effect, ordinarily accompanying enlargement of microvascular luminal diameter, augmentation of peripheral blood flow and reduction in arterial blood pressure.

The results in Fig. 8 to Fig. 13 have revealed an explicit stimulating effect of chronic prazosin administration on the vascularized tissue regeneration in the rabbit ear chamber. In the result in Fig. 12, the relative vascular area (RA) was calculated as the product of the covered area (CA) and the mean vascular density (MD); RA = CA x MD (Eq. 7). This estimation of RA involved a slight theoretical inconsistency, since CA was evaluated as the relative area covered by tissue to the ingrowable disk window of 6 mm in diameter, whereas MD was estimated as the vascular density in the covered area within the square grid of 5 mm x 5 mm, printed in the center of the window. Although accurate quantification of MD value required its measurement within the grid for precise allocation of the vasculature, the vascular density in the entire window might differ from the present

MD data evaluated in the grid, because the regeneration of the vascularized tissue always started from the marginal part of the window. The area covered by the grid (25 mm^2), however, occupied the major portion of the observing window (28.3 mm^2), as shown in Fig. 13. Accordingly, the errors which might be similarly involved in the present RA estimates of the prazosin-treated and control groups may not be regarded as a seriously disturbing factor. At least, the difference in RA values between the two groups in Fig. 12 is considered to be a reliable measure reflecting the integrity of increased diameter, length and number of microvessels by this vasodilator administration.

MD values seemed to be influenced by vascular tonus (vasoconstricted and/or vasodilated condition). To exclude this concern, we have comparatively investigated morphometric parameters under maximal vasodilated condition by warming the rabbit ear at 40℃ using infrared lamp (NM221BZ, National, Japan). The data (not shown) of this pilot study also exhibited significant difference between two groups.

To evaluate the peripheral blood flow condition, the red cell flow velocity was measured in venules by the dual window method in this study since it has been observed that new microvessels appear to sprout initially from venules and capillaries in vivo (D' Amore and Thompson, 1987, Myrhage and Hudlicka, 1978), not from arterioles. Unfortunately, the velocity measurement in arterioles was not possible by this method, because the arteriolar velocity often exceeded the upper limit of the velocity measurement (2 mm/s). The acute vasodilating effect of prazosin examined in the chamber of untreated animals revealed that its intravenous infusion in a comparable dose to the oral uptake increased the red cell velocity approximately by 1.35 times and enlarged the venular diameter nearly by 1.28 folds, simultaneously reducing the systemic arterial pressure by 32 %, compared to the preceding control state. These data suggest that the blood flow rate through venules was augmented by 2.2 times. The vasodilator administration has also been reported to associate a slight elevation of the venular pressure (Tillmans, et al., 1981). These effects of prazosin on microcirculation might not diminish so much even in

its long-term administration. According to the report by Dawson and Hudlicka (Dawson and Hudlicka, 1989) the capillary blood flow rates per cross sectional area of tissue in the tibialis anterior and soleus muscles of the prazosin-treated rats at the stage of 5 weeks can be estimated to be 1.77 and 1.35 times as much as those of the control rats respectively, if calculated from their data of capillary density and of single capillary flow measured following its oral administration, probably in the same dose as this study. The result in Fig. 15 shows that the average of red cell velocity in the prazosin-treated group at 9 POD was approximately 1.5 times as much as that in the control group at the venules of comparable diameters (Fig. 14). As for the later stages, the quantitative estimation of peripheral blood flow rate was rather difficult, because MD values of the two groups significantly differed due to cumulative changes in the microvascular morphology. It is likely that the associated variations in hemodynamic stresses might have affected the progress of vascularized tissue regeneration in the ear chamber in the two groups.

Among the rheological components, wall shear stress is thought to play the most significant role in physiological adaptation of the vascular system. Shear stress is imparted to the wall of a blood vessel as a result of the viscous drag associated with blood flow. The endothelial cells have a variety of proliferative (Ando, et al., 1990, Davies, et al., 1986, Eskin, et al., 1982), synthetic (Ando, et al., 1994, Rubanyi, et al., 1986), secretory (Diamond, et al., 1989), and self-adaptive capabilities (Eskin, et al., 1982, Franke, et al., 1984, Masuda and Fujiwara, 1993, Nerem, et al., 1981) that regulate vascular tonus, morphology, or adhesiveness. Recent evidence suggests that these functions are all affected by fluid shear stress on the endothelial wall. Wall shear stress is a regulating factor for adaptive vessel growth and angiogenesis (Ando and Kamiya, 1993, Kamiya and Ando, 1994, Kamiya, et al., 1994). Shear stress has also been suspected to play an important physiological role in capillary angiogenesis (Dawson and Hudlicka, 1993, Dawson and Hudlicka, 1989, Hudlicka, et al., 1992), since sustained increase in peripheral blood flow in muscles caused by repeated electrical nerve stimulation or by

chronic vasodilator administration stimulates capillary angiogenesis and increases capillary density, while reduced peripheral blood flow causes the size and number of arterioles to decrease (Wang and Prewitt, 1991). The results of these in vivo investigations suggest that the adaptive responses of large vessels and capillary angiogenesis are regulated by wall shear stress through the endothelium.

The levels of wall shear stress in venules were assessed from the data of red cell velocity and of vessel diameter by Eq. (8), assuming Poiseulle's flow. The validity of this assumption is somewhat questionable, because the flow of red cell suspension through a tube of 20 to 40 μm in diameter is known to exhibit non-Newtonian behavior and the velocity profile in the tube tends to deviate from the parabolic pattern of Poiseulle's flow (Chien, et al., 1984). In this study, however, the stress levels were evaluated in vessels of comparable diameters (Fig. 14), suggesting that the non-Newtonian effect must have been involved in each estimate virtually in the same extent. Accordingly, it is verified to compare the individual data between the prazosin-treated and control groups and between those at different PODs.

By comparing the results in Fig. 10 and in Fig. 16, it is evident that the differences in ingrowth rate of the vascularized tissue between the prazosin-treated and control groups were well correlated with those in wall shear stress at corresponding stages of the tissue repair process. Both were maximum at the early stage until 9 POD, moderate at the middle stage around 13 POD and minimum at the late stage after 21 POD. Together with these results, the transient changes in wall shear stress levels in Fig. 8 visualizes the shear-induced adaptive responses of the venules in the prazosin-treated group. The time course, gradually decreasing toward the control level, suggest the following process; 1) The increased peripheral blood flow by the treatment elevated the shear stress level at ingrowing microvessels at the early stage. 2) The elevated shear stress stimulated the proliferative activity of the microvessels to facilitate the vascularized tissue regeneration. 3) The augmented vascular bed in turn acted to reduce the stress level

of microvessels including venules in the later stages, until the shear stress approached the control physiological level and the entire remodeling process was completed. Such an autoregulatory mechanism in the stress-response relationship as observed in this study is one of major characteristics of the adaptive responses in the vascular system to wall shear stress as manifested in large arteries (Kamiya and Ando, 1995, Kamiya and Togawa, 1980, Langille and O' Donnell, 1986, Tohda, et al., 1992) and of other biological systems to specific mechanical stresses as well (Cowin, 1986, Lund and Thomanek, 1978).

In order to confirm this kind of biological feedback mechanisms, it is of essential importance to follow transient changes in the key stress during the remodeling process. In this aspect, it is not reasonable to suspect the role of a stress in an adaptive response from the information obtained only at a certain stage of the process, as done by Dawson and Hudlicka (Dawson and Hudlicka, 1989). These authors found a comparable shear stress level in the skeletal muscle capillary beds of prazosin-treated and untreated rats after 5 weeks of the oral administration and thereby concluded that the shear stress was not the key factor inducing the adaptive response in the capillary network. It is highly likely that the comparable shear stress was a consequence of the complete autoregulation in the shear-induced capillary angiogenesis, as clearly demonstrated from the results in venules at 21 POD in Fig. 16. However, the findings of this study present necessary but not sufficient conditions to conclude shear-induced mechanisms, since in this model there are multiple other factors that could have produced the remodeling in treated wounds: circumferential wall tension generated by blood flow, growth factors such as bFGF and PDGF released from endothelial cells, and the vasoactive substance and oxygen delivery. The mechanisms proposed here is one scenario that could consistently explain the obtained data.

With respect to the adaptive remodeling of terminal and arcade arterioles under vasodilated conditions, Price and Skalak (Price and Skalak, 1995, Price and Skalak, 1994) have recently claimed that the major role is played by the elevated circumferential

wall stress, but not by the wall shear stress, based on the theoretical predictions from a computer simulation model of the vascular network. These authors also showed experimental evidence that the same long-term prazosin treatment as this study brought about the development of the arteriolar segments in the rat gracilis muscle and concluded that the observed remodeling of arterioles was induced by the increased circumferential stress (Price and Skalak, 1996). Their original theoretical model (Price and Skalak, 1994), however, has been constructed under the assumption that in the arteriolar network, blood flow rate at each vascular branch is completely autoregulated to remain constant. This model is then limited in its application to autoregulated microvascular systems such as in the brain or kidney and is difficult to the systems like those in the skin and regenerating tissue. It is also not appropriate to expect that the theoretical predictions of this model can explain the experimental findings observed in such a situation as during prazosin treatment, because the peripheral blood flow has been confirmed to increase significantly, by the red cell velocity measurement in this study. This model should be extended, so that it may be applicable to more plausible hemodynamic situations under vasodilator effects or other physiological or pathological conditions.

As a matter of fact, it is difficult to predict the responses of these stresses against a vasodilator. The circumferential wall stress at an arteriole (σ) can be approximated as σ = Pr/h where P, r and h indicates hydrostatic pressure, vessel radius and wall thickness (Price and Skalak, 1994), whereas the wall shear stress (τ) is expressed as τ = (dP/dl)(r/2) in which dP/dl denotes pressure gradient at the arteriole (Stoke's equation). When a vasodilator like prazosin is administered, P and dP/dl are usually reduced, r is increased and h is decreased in inverse proportion to r to conserve the wall mass. It is then obvious that, whether σ or τ is increased or decreased, depends upon whether the reduction in P or in dP/dl is compensated by the increase in r or not. Quantitative in vivo data are lacking concerning these responses, to identify which stress is playing a major role in the arteriolar adaptive remodeling induced by the vasodilator treatment.

Besides such pharmacological information, it is also important to quantify the temporary changes in the stress level during the chronic adaptive response, as performed in the present study for the venular shear stress. With respect to the arteriolar wall shear stress, it is possible to follow its transient alterations in the rabbit ear chamber by employing the non-invasive technique of microscopic laser Doppler flowmetry (Seki, 1990) designed for higher red cell velocity measurement. As for the circumferential wall stress estimation, the technique of local pressure measurement by microvessel compression (Hori, et al., 1983) may be useful in the skinfold chamber in rats. Further studies are required to shed light into the above ambiguity.

Conclusion

Chronic administration of α-1 blocker, prazosin induced increase in wall shear stress in microvessels and stimulated the angiogenic response in the rabbit ear chamber. Elevated shear stress gradually down regulated toward the control level during acceleration of angiogenesis. This study has provided experimental evidence that angiogenesis during tissue repair is governed by the shear stress dependent adaptive response of the vascular system.

References

1. Ando, J., and A. Kamiya. (1993). Blood flow and vascular endothelial cell function. *Front. Med. Biol. Engng.* 5, 245-264.
2. Ando, J., T. Komatsuda, C. Ishikawa, and A. Kamiya. (1990). Fluid shear stress enhanced DNA synthesis in cultured endothelial cells during repair of mechanical denudation. *Biorheology* 27, 675-684.
3. Ando, J., T. Komatsuda, and A. Kamiya. (1988). Cytoplasmic calcium response to fluid shear stress in cultured vascular endothelial cells. *In Vitro Cell. Dev. Biol.* 24, 871-7.
4. Ando, J., A. Ohtsuka, R. Korenaga, and A. Kamiya. (1991). Effect of extracellular ATP level on flow-induced Ca^{++} response in cultured vascular endothelial cells. *Biochem. Biophys. Res. Commun* 179, 1192-9.
5. Ando, J., A. Ohtsuka, R. Korenaga, T. Kawamura, and A. Kamiya. (1993). Wall shear stress rather than shear rate regulates cytoplasmic Ca^{++} responses to flow in vascular endothelial cells. *Biochem. Biophys. Res. Commun* 190, 716-23.
6. Ando, J., H. Tsuboi, R. Korenaga, Y. Takada, N. Toyama-Sorimachi, M. Miyasaka, and A. Kamiya. (1994). Shear stress inhibits adhesion of cultured mouse endothelial cells to lymphocytes by downregulating VCAM-1 expression. *Am. J. Physiol.* 267, C679-87.
7. Asano, M., K. Yoshida, and K. Tatai. (1963). Observation of the behavior of microcirculation by rabbit ear chamber technique. I. *Bull. Inst. Publ. Health.* 12, 34-44.
8. Baba, K., T. Kawamura, M. Shibata, M. Sohirad, and A. Kamiya. (1995). Capillary-tissue arrangement in the skeletal muscle optimized for oxygen transport in all mammals. *Microvasc Res* 49, 163-179.
9. Chien, S., S. Usami, and R. Skalak. (1984). Blood flow in small tubes. In "*Handbook of Physiology* " (E. M. Renkin and C. C. Michel, eds.), pp. 217-

249. American physiological society, Bethesda, Maryland.

10. Clark, E. R., W. J. Hitschler, H. T. Kirby-Smith, and J. H. Smith. (1931). General observations on ingrowth of new blood vessels into standerdized chambers in rabbit's ear, and subsequent changes in newly grown vessels over period month. *Anat.Rec.* 50, 129-167.
11. Cliff, W. J. (1965). Kinetics of wound healing in rabbit ear chambers, a time lapse cinemicroscopic study. *Quart. J. Exp. Physiol. Cog. Med. Sci.* 50, 79-89.
12. Cowin, S. C. (1986). Wolff's law of trabecular architechture at remodeling equilibrium. *J. Biomech. Eng.* 108, 83-88.
13. D' Amore, P. A., and R. W. Thompson. (1987). Mechanisms of angiogenesis. *Annu. Rev. Physiol.* 49, 453-464.
14. Davies, P. F., A. Remuzzi, E. J. Gordon, C. F. Dewey, Jr., and M. A. Gimbrone, Jr. (1986). Turbulent fluid shear stress induces vascular endothelial cell turnover in vitro. *Proc. Natl. Acad. Sci. USA* 83, 2114-2117.
15. Dawson, J. M., and O. Hudlicka. (1993). Can changes in microcirculation explain capillary growth in skeletal muscle ? *Int. J. Exp. Path.* 74, 65-71.
16. Dawson, J. M., and O. Hudlicka. (1989). The effects of long term administrarion of prazosin on the microcirculation in skeletal muscles. *Cardiovas. Res.* 23, 913-920.
17. Diamond, S. L., S. G. Eskin, and L. V. McIntire. (1989). Fluid flow stimulates tissue plasminogen activator secretion by cultured human endothelial cells. *Science* 243, 1483-5.
18. Dudar, T. E., and R. K. Jain. (1983). Microcirculatory flow changes during tissue growth. *Microvasc.Res.* 25, 1-21.
19. Ebert, R. H., H. W. Florey, and B. D. Pullinger. (1939). A modification of a Sandison-Clark chamber for observation of transparent tissue in the rabbit's ear. *J.Pathol.Bacteriol.* 48, 79-94.

20. Eskin, S. G., H. D. Sybers, W. O'Bannon, and L. T. Navarro. (1982). Performance of tissue cultured endothelial cells. *Artery* 10, 159-171.

21. Franke, R. P., M. Grafe, H. Schnittler, D. Seiffge, and C. Mittermayer. (1984). Induction of human vascular endothelial stress fibres by fluid shear stress. *Nature* 307, 648-649.

22. Hori, K., M. Suzuki, I. Abe, S. Saito, and H. Sato. (1983). A micro-occlusion technique for measurement of the microvascular pressure in tumor and subcutis. *Gann* 74, 122-127.

23. Hsieh, H. J., N. Q. Li, and J. A. Frangos. (1991). Shear stress increases endothelial platelet-derived growth factor mRNA levels. *Am. J. Physiol.* 260, H642-646.

24. Hudlicka, O., M. Brown, and S. Egginton. (1992). Angiogenesis in skeletal and cardiac muscle. *Physiol. Rev.* 72, 369-417.

25. Intaglietta, M., N. R. Silverman, and W. R. Tompkins. (1975). Capillary flow velocity measurement in vivo and in situ by television methods. *Microvas Res* 10, 165-179.

26. Johnson, P. C. (1986). Flow measurement technique in the microcirculation. In "*Microcirculatory technology* " (C. H. Baker and W. L. Nastuk, eds.), pp. 149-160. Academic press, Inc., Orlando, Florida.

27. Kamiya, A., and J. Ando. (1994). Fluid shear stress and vascular endothelial cell biomechanics. In "*Clinical biomechanics and related research* " (Y. Hirasawa, C. B. Sledge and S. L.-Y. Woo, eds.), pp. 255-271. Springer-Verlag, Tokyo.

28. Kamiya, A., and J. Ando. (1995). Responses of vascular endothelial cells to fluid shear stress: Mechanism. In "*Biomechanics-Functional Adaptation and Remodeling*" (K. Hayashi, A. Kamiya and K. Ono, eds.), pp. 29-56. Springer-Verlag, Tokyo.

29. Kamiya, A., R. Korenaga, and J. Ando. (1994). Endothelial cell responses to fluid shear stress. In "*Endothelium-derived factors and vascular functions* " (T.

Masaki, eds.), pp. 103-112. Elsevier Science publishers B.V., Amsterdam.

30. Kamiya, A., and T. Togawa. (1980). Adaptive regulation of wall shear stress to flow change in the canine carotid artery. *Am. J. Physiol.* 239 (Heart Circ. Physiol. 8), H14-H21.
31. Langille, B. L., and F. O'Donnell. (1986). Reductions in arterial diameter produced by chronic decreases in blood flow are endothelium-dependent. *Science* 231, 405-407.
32. Lund, D. D., and R. J. Thomanek. (1978). Myocardial morphology in spontaneously hypertensive and aortic-constricted rats. *Am. J. Anat.* 152, 141-152.
33. Masuda, M., and K. Fujiwara. (1993). Morphological responses of single endothelial cells exposed to physiological levels of fluid shear stress. *Front. Med. Biol. Eng.* 5, 79-87.
34. Myrhage, R., and O. Hudlicka. (1978). Capillary growth in chronically stimulated adult skeletal muscle as studied by intravital microscopy and histological methods in rabbits and rats. *Microvasc. Res.* 16, 73-90.
35. Nerem, R. M., M. J. Levesque, and J. F. Cornhill. (1981). Vascular endothelial morphology as an indicator of the pattern of blood flow. *J. Biomech. Eng.* 103, 172-176.
36. Price, R. J., and T. C. Skalak. (1996). Chronic α_1-adrenergic blockade stimulates terminal and arcade arteriolar development. *Am. J. Physiol. (Heart Circ. Physiol. 40)* 271, H752-H759.
37. Price, R. J., and T. C. Skalak. (1995). A circumferential Stress-growth rule predicts arcade arteriole formation in a network model. *Microcirculation* 2, 41-51.
38. Price, R. J., and T. C. Skalak. (1994). Circumferential wall stress as a mechanism for arteriolar rarefaction and proliferation in a network model. *Microvas. Res.* 47, 188-202.

39. Rubanyi, G. M., J. C. Romero, and P. M. Vanhoutte. (1986). Flow-induced release of endothelium-derived relaxing factor. *Am. J. Physiol.* 250, H1145-9.

40. Sandison, J. C. (1928). The transparent chamber of rabbit's ear, giving a complete description of improved technique of construction and introduction and general account of growth behavior of living cells and tissues as seen with microscope. *Amer.J.Anat.* 41, 447-473.

41. Seki, J. (1990). Fiber-optic laser-Doppler anemometer microscope developed for the measurement of microvascular red cell velocity. *Microvasc. Res.* 40, 302-316.

42. Thoma, R. (1911). Uber die Histomechanik des Gefassystems und die Pathogenese der Angiosklerose. *Pathol Anat Physiol* 204, 1-74.

43. Tillmans, T. H., A. M. Dart, N. Parekh, F. J. Neumann, P. Moller, R. Zimmerman, M. Steinhausen, and W. Kubler. (1984). Calcium antagonists(nifegipine) and coronary vasodilators(dipyridamole)-different effects on small coronary resistance vessels (Abstract). *Int. J. Microcirc. Clin. Exp.* 3, 342.

44. Tillmans, T. H., M. Steinhausen, H. Leinberger, H. Thederan, and H. Kubler. (1981). Pressure measurement in the terminal vascular bed of the epimyocardium of rats and cats. *Circ. Res.* 49, 1202-1211.

45. Tillmans, T. H., M. Steinhausen, H. Thederan, and N. Parekh. (1977). In vivo microscopic studies of the ventricular microcirculation of the rat heart. *J. Mol. Cell. Cardiol.* 9, Suppl., 57-58.

46. Tohda, K., H. Masuda, K. Kawamura, and T. Shozawa. (1992). Difference in dilatation between endothelial-preserved and -desquamated segments in the flow loaded rat common carotid artery. *Arterioscler. Thomb.* 12, 519-528.

47. Van Den Brenk, H. A. S. (1956). Studies in the restorative growth processes in mammalian wound healing. *Brit.J.Surg.* 43, 535-546.

48. Wang, D. H., and R. L. Prewitt. (1991). Microvascular development during normal growth and reduced blood flow: introduction of a new model. *Am. J.*

Physiol. 260 (Heart Circ. Physiol. 29), H1966-H1972.

49. Yang, W., J. Ando, R. Korenaga, T. Toyo-oka, and A. Kamiya. (1994). Exogenous nitric oxide inhibits proliferation of cultured vascular endothelial cells. *Biochem. Biophys. Res. Commun.* 203, 1160-1167.
50. Yoshizumi, M., H. Kurihara, T. Sugiyama, F. Takaku, M. Yanagisawa, T. Masaki, and Y. Yazaki. (1989). Hemodynamic shear stress stimulates endothelin production by cultured endothelial cells. *Biochem. Biophys. Res. Commun.* 161, 859-64.
51. Zawicki, D. F., R. K. Jain, G. W. Schmid-Schoenbein, and S. Chien. (1981). Dynamics of Neovascularization in normal tissue. *Microvasc. Res.* 21, 27-47.
52. Ziada, A., O. Hudlicka, and K. R. Tyler. (1989). The effect of long-term administration of a1 blocker prazosin on capillary density in cardiac and skeletal muscle. *Pfluegeres Arch.* 415, 355-360.

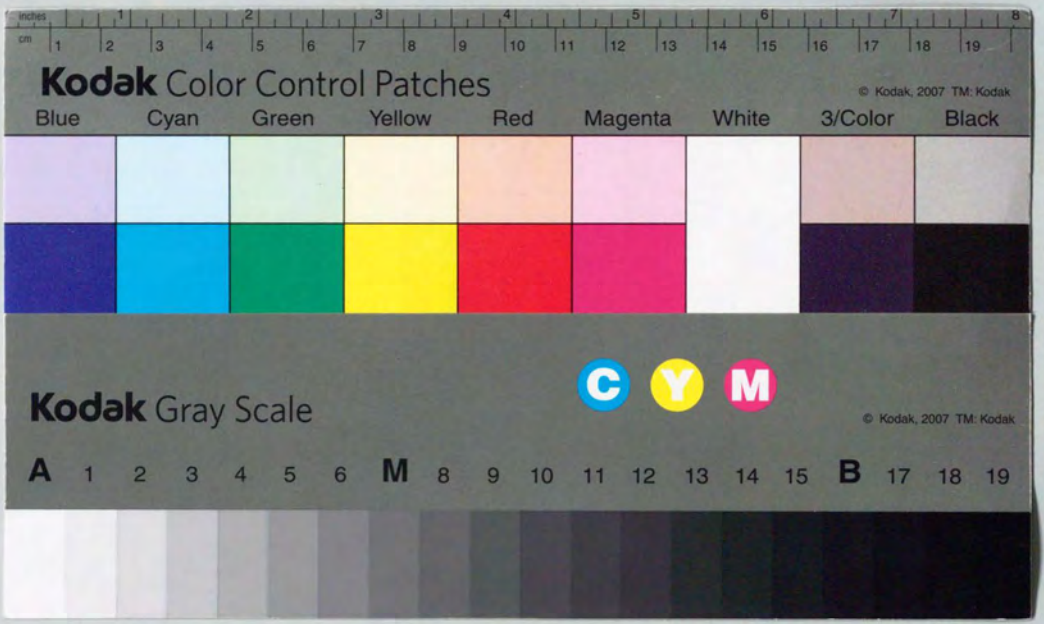
inches
cm
Kodak Color Control Patches
© Kodak, 2007 TM: Kodak
Blue
Cyan
Green
Yellow
Red
Magenta
White
3/Color
Black
Kodak Gray Scale
C
Y
M
© Kodak, 2007 TM: Kodak
A 1 2 3 4 5 6 M 8 9 10 11 12 13 14 15 B 17 18 19